Am J Nucl Med Mol Imaging 2021;11(4):250-259
www.ajnmmi.us /ISSN:2160-8407/ajnmmi0133241

Original Article

Amino acid transporter expression and 18F-FACBC uptake at PET in primary prostate cancer

Andreas J Tulipan[1,2], Unn Beate Salberg[3,2], Knut Håkon Hole[1,2], Ljiljana Vlatkovic[4], Eva-Katrine Aarnes[3], Mona-Elisabeth Revheim[1,2], Heidi Lyng[3,5], Therese Seierstad[1]

[1]Division of Radiology and Nuclear Medicine, Oslo University Hospital, Oslo, Norway; [2]Institute of Clinical Medicine, University of Oslo, Oslo, Norway; [3]Department of Radiation Biology, Institute for Cancer Research, Oslo University Hospital, Radiumhospitalet, Oslo, Norway; [4]Department of Pathology, Oslo University Hospital, Oslo, Norway; [5]Department of Physics, University of Oslo, Oslo, Norway

Received March 17, 2021; Accepted June 25, 2021; Epub August 15, 2021; Published August 30, 2021

Abstract: Little is known about the transport mechanism of *anti*-3-18F-fluorocyclobutane-1-carboxylic acid (FACBC) into prostate tumors. Because of the structural similarity to natural amino acids, FACBC is anticipated to cross the cell membrane via amino acid transporters, and preclinical studies have suggested that ASCT2, LAT1 and SNAT2 are involved. In 16 patients with intermediate or high-risk prostate cancer we matched the FACBC uptake from clinical PET to the location of punch biopsies from resected prostatectomy specimens and compared maximum standardized uptake value (SUVmax) with the gene expression of 40 amino acid transporters. The study also included immunohistochemistry for the three amino acid transporters ASCT2, LAT1 and SNAT2. Furthermore, we performed global gene expression analysis of the biopsies to investigate biological processes associated with FACBC uptake. Several amino acid transporters had a higher gene expression level than the others, but we found no significant correlations between SUVmax and the gene expression levels of any of 40 different amino acid transporters. In the immunohistochemical analyses, ASCT2 and SNAT2 were highly expressed, but not correlated to SUVmax. LAT1 had low gene- and protein expression. Global gene expression analyses identified 153 unique genes that were positively correlated to SUVmax. These genes were found to be associated with gene sets reflecting intracellular transport and high metabolic activity. Based on the study findings we propose that the uptake mechanism of FACBC is more complex than mediated by a few amino acid transporters.

Keywords: Prostate carcinoma, fluciclovine, FACBC, amino acid transport, gene expression profiling, immunohistochemistry

Introduction

The radiolabeled synthetic amino acid analogue *anti*-3-18F-fluorocyclobutane-1-carboxylic acid (FACBC) was in 2016 approved by the U.S. Food and Drug Administration and in 2017 by the European Medicines Agency as a PET tracer for patients with suspected prostate cancer recurrence (https://www.ema.europa.eu/medicines/human/EPAR/axumin, https://www.fda.gov/newsevents/newsroom/pressannouncements/ucm503920.htm). FACBC is a non-metabolized non-natural amino acid analogue that has early uptake in tumor tissue and low urinary excretion [1-3]. Little is known about the transport mechanism of FACBC into prostate tumors. Because of the structural similarity to natural amino acids, FACBC is anticipated to cross the cell membrane via amino acid transporters. Our knowledge arises mainly from *in vitro* studies performed by a Japanese group. Their studies in the human prostate cancer cell line DU145 suggested that FACBC-uptake was mainly mediated by Na^+ dependent amino acid transporters [2]. Transporter knockdown assays of the two major transporters, the Na^+ coupled amino acid transporter 2 (SNAT2) and the alanine-serine-cysteine transporter 2 (ASCT2), suggested that ASCT2 was an important transporter for FACBC in this cell line. By using several human prostate cancer cell lines, the Na^+ independent large neutral amino acid transporter (LAT1) was also identified as a FACBC transporter [4]. LAT1 forms a heteromeric trans-

Table 1. Patient and tumor characteristics

Patient	Age [years]	PSA [ng/mL]	Prostate volume[a] [ml]	Pathological T stage	Gleason score[b]	ISUP Grade Group[e]
1	70	8.7	52	T3a	8	4
2	61	9.3	32	T2c	8	4
3[c]	58	12	39	T3a	7b	3
4[c]	60	8.7	31	T3a	7b	3
5[c]	74	4.7	48	T3a	7a	2
6	66	11	40	T3a	7a	2
7	68	5	24	T3a	8	4
8	57	9.1	57	T3a	7a	2
9	58	4.6	44	T2c	6	1
10[c]	66	7.1	42	T3a	7a	2
11	73	8.3	43	T2c	6	1
12[c]	68	37	57	T3b	7a/7b[d]	2/3[d]
13	71	8.4	58	T2a	7a	2
14[c]	71	16	46	T3b	7b/8[d]	3/4[d]
15	65	12	47	T3a	7a	2
16	59	5.4	39	T3a	7b	3

a, Prostate volume calculated from MRI; b, Gleason score in the punch biopsies according to the updated Gleason grading system from 2010; c, Patients with two biopsies from the tumor; d, Different Gleason score in the two biopsies; e, ISUP grade groups corresponding to the original Gleason scores.

porter complex with 4F2 cell-surface antigen heavy chain (4F2HC) that is essential for the LAT1 stability and for its localization to the plasma membrane [5, 6]. In a study of Xenopus laevis oocytes, both ASCT2 and SNAT2 recognized anti-FACBC as a substrate [7].

In prostate tumors in patients, elevated expression of ASCT2 and LAT1 has been associated with aggressive disease [8, 9]. Contrary to the data from the cell line studies, Saarinen *et al.* found no correlation between ASCT2 expression and FACBC uptake at PET in a group of 24 prostate cancer patients [10]. Moreover, ASCT2 expression showed no difference between tumors with different Gleason grade groups. For LAT1, the expression increased with increasing Gleason grade, and for early time points after FACBC administration there was a significant higher LAT1 expression in the tumors with highest FACBC-uptake [10]. To the best of our knowledge, no studies have been conducted in patients to analyze FACBC uptake at PET against global gene expression data. This approach enables studies of all genes in the genome and provides information about amino acid transporters that may be linked to the transport of FACBC into prostate cancer. Information about biological processes associated with FACBC uptake may also be achieved.

In the present study we aimed to investigate the FACBC uptake mechanism in prostate cancer patients by comparing FACBC PET data with gene- and protein expression in punch biopsies from the tumors, using a strategy to match biopsy locations and image regions. We investigated the gene expression of 40 amino acid transporters that have been detected in prostate cancer specimens [2]. In particular, we focused on ASCT2, LAT1 and SNAT2 that have been linked to FACBC uptake in preclinical studies [2, 4, 7]. We also performed global gene expression analyses of the same biopsies to search for biological processes associated with increased FACBC uptake.

Materials and methods

Patient cohort

Sixteen prostate cancer patients, referred to our institution for prostatectomy between February 2013 and May 2016, were included in this prospective study (ClinicalTrials.gov Identifier: NCT01464216). The Regional Committee for Medical and Health Research Ethics approved the study (REC 2010/1656). All patients gave written informed consent prior to study inclusion. Patient and tumor characteristics are summarized in **Table 1**.

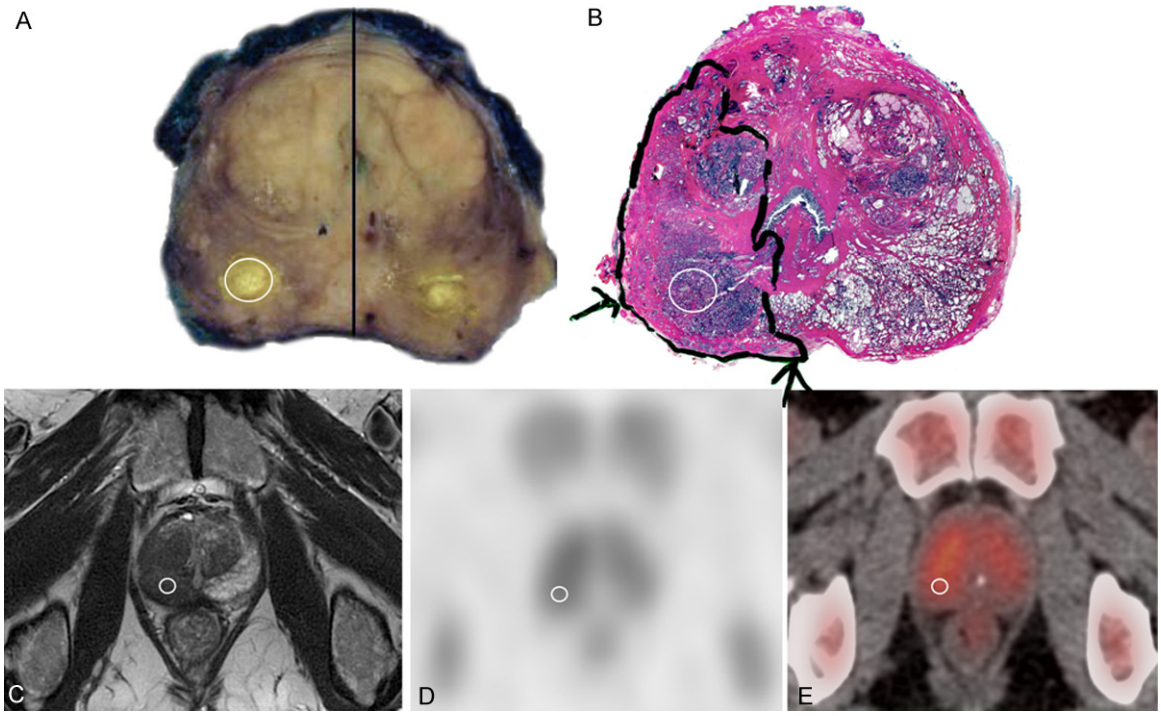

Figure 1. Method used to match punch biopsy location and FACBC PET image region. A. The resected prostate gland showing the location of the punch biopsies (white circle). B. HE-stained whole-mount section with the tumor outlined. C. Axial T2-weighted MR image. D. FACBC PET image with the biopsy region of interest. E. Fused FACBC PET/CT image.

FACBC PET/CT

For all included patients FACBC PET/CT was performed less than 18 days (range; 1-18, mean; 9.4, standard deviation (SD); 5.7) prior to prostatectomy. The PET/CT images were obtained with a Biograph40 mCT (Siemens, Erlangen, Germany). The patients were instructed to fast for at least four hours and to void the bladder before the examination. First, a helical CT scan (field of view (FOV) = 78 cm, tube voltage = 120 kV, CareDose 4D eff. 82 mAs, slice thickness = 1.5 mm, matrix size = 512 × 512) of the pelvis was acquired for attenuation correction. Following intravenous bolus administration of 281-301 MBq FACBC and saline flush of 10-20 ml, a 14-minutes list-mode PET acquisition of one bed position (FOV of 21.6 cm centered above the symphysis, FOV = 70 cm) was obtained. The list-mode data were re-binned into seven image time frames of 2 minutes. The resulting sinograms were reconstructed using 3D iterative ordered-subset expectation maximization (OSEM) with 2 iterations and 21 subsets, time of flight (TOF), point-spread function (PSF)-correction, slice thickness 1.5 mm, matrix size 128 × 128, and a Gaussian post-reconstruction convolution kernel with full width at half maximum (FWHM) of 3 mm. The PET images had a voxel size of 6.3 mm × 6.3 mm × 1.5 mm. All images were transferred to a remote computer for further analysis.

Tumor biopsies

By guidance from multiparametric MRI, preoperative biopsies and palpation of the resected specimen, the prostate gland was cut horizontally into two halves at the site where the tumor was assumed to be located (**Figure 1**). Punch biopsies with a diameter of 6 mm were taken from the tumor and immediately snap frozen in liquid nitrogen and stored at -80°C. For some patients, tumor biopsies were obtained from both halves of the prostate. After excluding biopsies with less than 50% tumor cells, a total of 22 biopsies from 16 patients remained for the analyses.

After biopsy collection, the gland was fixed in 10% buffered formaldehyde for at least two days. Grossing was performed according to a

standardized protocol where total prostate with seminal vesicles were embedded [11]. The apex and the base of the prostate were cut as sagittal sections using the cone method. The remaining body was cut into 3-4 mm transverse slices and prepared as whole-mount sections. The sections were stained with hematoxylin and eosin (HE) and examined by an experienced uropathologist (L.V.). Histopathological assessment included staging according to the 7th edition TNM classification [12] and determination of Gleason score in the biopsies [13].

Analyses of the FACBC PET/CT images

Image analyses were performed with OsiriX MD (OsiriX MD v.10.0.0, Pixmeo SARL, Bern, Switzerland). A nuclear radiologist (A.J.T.), with five years of experience in FACBC PET prostate imaging, placed a 6 mm circular region of interest (ROI) in the FACBC PET image corresponding to the location of the punch biopsy (**Figure 1**). The placement of the ROI was guided by photographs of the sliced prostate gland showing the bio-banked areas, whole-mount HE-stained sections, MR images, PET/CT images and anatomical landmarks, such as seminal vesicles, ejaculatory ducts, relative distance from the prostatic capsule, and midline. The standardized uptake value (SUV) was calculated by dividing the voxel signal intensity by the injected activity per body weight, and the maximum value (SUVmax) within the ROI was used in the further analyses.

Gene expression analyses

Gene expression profiling of the 22 biopsies from the 16 patients was derived using Illumina bead arrays HT-12 v4 (Illumina Inc, San Diego, CA, USA) with 47323 probes. For tumors with two biopsies, the average expression value of the biopsies was used for each probe. From the fresh frozen biopsies, 10 slices of 20 μm thickness were obtained for RNA isolation. This resulted in totally 1 mm tumor tissue with approximately 6 mm in diameter. MiRNeasy MiniKit (Qiagen, Hilden, Germany) was used for isolation of total RNA. RNA quality control was performed using Agilent 2100 Bioanalyzer (Agilent Technology, Santa Clara, CA, USA). cRNA was synthetized, labelled and hybridized to the arrays. The software provided by the manufacturer (Illumina Inc, San Diego, CA, USA) was used for signal extraction and quantile normalization. Poorly expressed transcripts; i.e. probes with a signal lower than two times the background signal in more than 12 patients, were excluded. Moreover, for probes representing the same gene, the probe with highest interquartile range was used. This pre-processing procedure led to expression values for 10192 genes. Log2-transformed data were used in the further analyses.

Immunohistochemistry

Immunohistochemistry was performed with the polyclonal rabbit antibodies ASCT2 (1:500, Sigma-Aldrich) and SNAT2 (1:50, Sigma-Aldrich) on 22 biopsies from the 16 patients. In biopsies from four tumors, the polyclonal antibody LAT1 (1:35, Sigma-Aldrich) was used to evaluate a possible LAT1 protein expression. After thawing, sections were fixed in formalin for 15 minutes and rinsed in running water. Antigen retrieval was performed through boiling in citrate buffer (pH 6.0) in a microwave oven for 20 minutes. Endogenous tissue peroxidase was quenched with hydrogen peroxide before incubation with antibodies for 30 minutes in room temperature. For visualization, Envision™ system (Dako) was used, followed by counterstaining with haematoxylin, dehydration and mounting. The staining pattern of the tumors was evaluated blinded to gene expression and scored by a pathologist (L.V.). Only membrane staining was evaluated, and the immunohistochemistry-sections were graded according to staining extent (1: <50%, 2: 50-75%, 3: >75%) and intensity (1: light, 2: moderate, 3: strong). For patients with two tumor biopsies, the mean value of the two biopsies was used. For comparing protein expression to gene expression and FACBC uptake, an immunoscore was calculated as the product of staining extent and staining intensity, ranging from 1 × 1 to 3 × 3.

Data analyses

For statistical analyses, R software packages (version 3.5.1, Boston MA, USA) and IBM SPSS Statistics (version 27, Armonk NY, USA) were used. Relationships between gene expression and SUVmax, for the time intervals 2-4 and 4-6 minutes, were investigated with Spearman's rank correlation analysis for 40 amino acid transporters. We also generated a total amino acid transporter gene score by combining the gene expression of all 40 amino acid transport-

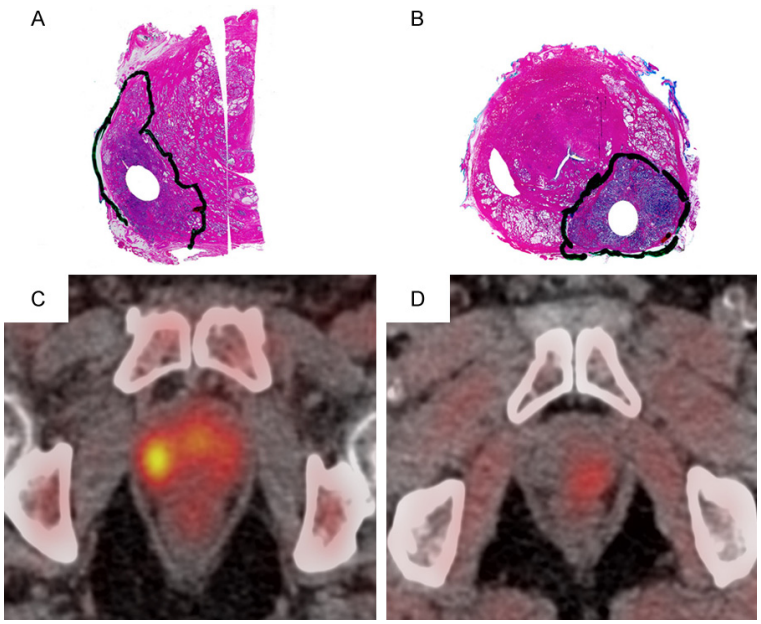

Figure 2. Example of tumors with high (left) and low (right) SUVmax. Upper row shows HE-stained whole-mount sections. The tumors are outlined in black. The white ellipsoids within the tumors represent the site of the punch biopsies. Lower row shows the corresponding fused FACBC/CT-images with SUV scale ranging from 0 (no color) to 20 (yellow).

ers, to investigate a possible relationship to SUVmax. The transporter gene score was calculated by averaging the median centered expression levels of the 40 amino acid transporter genes, as described by Ragnum and colleagues [14]. The significance level was set to 0.05.

To investigate biological processes associated with FACBC uptake, Spearman correlation analysis was used to identify a list of genes in which the gene expression level was significantly correlated to SUVmax. Gene set enrichment analysis (GSEA) was performed for the strongest correlated genes in the list. A computational methodology identifies overlap between the list of correlating genes and predefined gene sets. Hallmark gene sets represent specific biological states and ontology gene sets represent biological processes. The output from GSEA is the probability (*P*-value) that the overlap between the upregulated genes in our patient data and the predefined gene sets are different from chance using the Benjamini-Hochberg correction (https://www.statisticshowto.com/benjamini-hochberg-procedure/) to control the false discovery rate (FDR) An FDR cut-off of q = 0.05 was considered significant.

Results

FACBC uptake

Mean tumor SUVmax for 2-4- and 4-6-minutes post injection of FACBC were 6.4 (range; 3.2-12, SD; 2.5) and 6.3 (range; 2.9-12.5, SD; 2.8), respectively. There was a large variation in SUVmax between patients, but no significant difference in SUVmax between 2-4 and 4-6 minutes (P = 0.81). **Figure 2** shows one patient with low uptake and one patient with high uptake of FACBC in the tumor.

Gene expression of amino acid transporters

Figure 3 shows the gene expression level for 40 amino acid transporters that have been detected in prostate cancer [2]. Eight transporters including *LAT2*, *CAT2*, *CAT1*, *4F2HC*, *SNAT2*, *SNAT1*, *PAT1* and *ASCT2* showed a higher expression level than the others. The gene expression of individual tumors is shown in Supplementary Table 1.

Correlation between FACBC uptake and gene expression of the amino acid transporters

Figure 4 shows the FACBC uptake for individual patients sorted from lowest to highest SUVmax at 4-6 minutes and gene expression levels for *ASCT2*, *LAT1* and *SNAT2* in the same order. The *LAT1* expression level was comparable to the background noise and was excluded from the correlation analysis against SUVmax.

Spearman correlation coefficients and corresponding *P*-values from the comparison of SUVmax with expression of *ASCT2*, *SNAT2,* and the transporter gene score are shown in **Table 2.** The correlation results for each of the 40 amino acid transporters are included in Supplementary Table 2.

We found no significant positive correlations between SUVmax and the gene expression levels for any of the 40 amino acid transporters or the transporter gene score. FACBC uptake

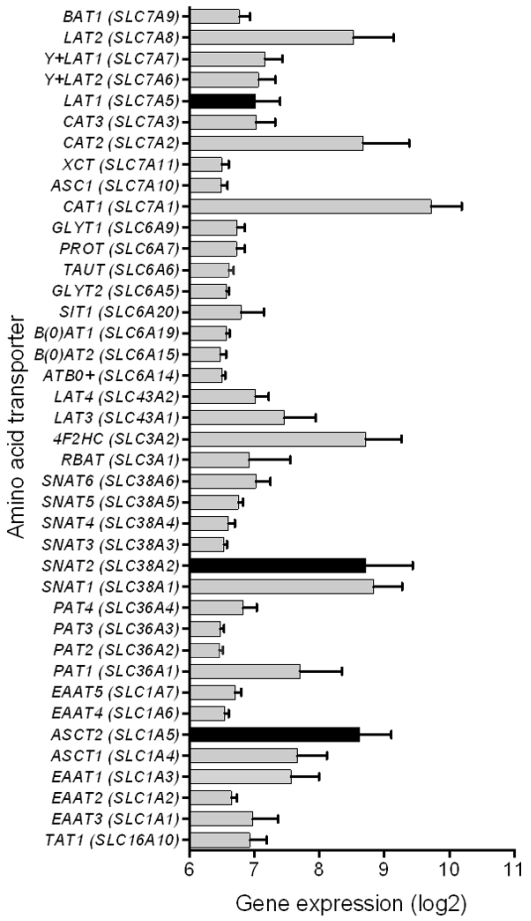

Figure 3. Gene expression levels of amino acid transporters in prostate cancer specimens. The columns represent mean values and the bars standard deviation. *LAT1*, *ASCT2*, and *SNAT2* are shown with black bars. Official gene symbols are shown in parentheses.

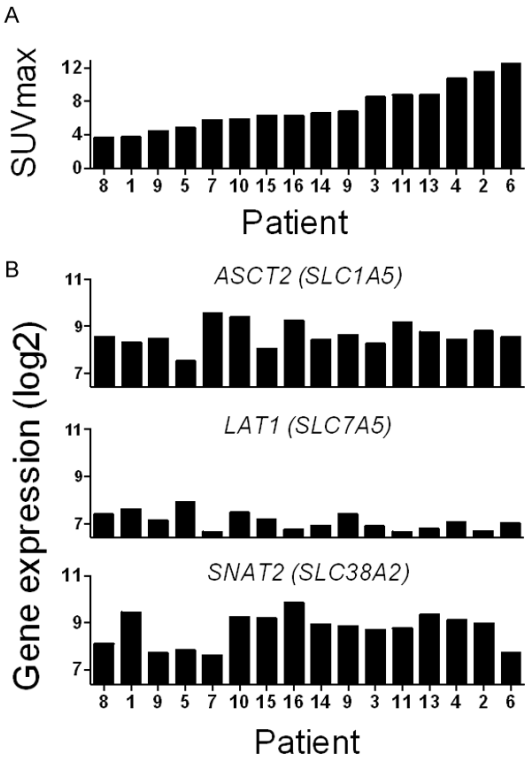

Figure 4. SUVmax at 4-6 minutes (A) and gene expression of *ASCT2*, *LAT1* and *SNAT2* for 16 patients (B). The patients are ordered from left to right according to increasing SUVmax at 4-6 minutes. Official gene symbols are shown in parentheses.

quantification using SUVmean yielded similar correlations to gene expression as using SUVmax (data not shown).

Correlation between FACBC uptake and protein expression of ASCT2 and SNAT2

Examples of immunohistochemical staining of ASCT2 and SNAT2 are shown in **Figure 5**, whereas the immunoscores for individual patients are shown in **Table 3**. Whereas the ASCT2 positive cells had predominantly membrane staining, SNAT2 had significant cytoplasmic staining as well. In accordance with the gene expression data, the LAT1 expression was low, and mainly seen in the cytoplasm. Consequently, an immunoscore was not calculated for this protein.

The immunoscores of ASCT2 and SNAT2 were analyzed against gene expression level and SUVmax (**Table 4**). There was no significant correlation between the immunoscores of either ASCT2 or SNAT2, and SUVmax at any time points. We found a significant positive correlation between the immunoscore and gene expression level for ASCT2, but not for SNAT2.

GO terms and hallmarks associated with FACBC uptake

Significant positive correlations (nominal $P < 0.05$) between SUVmax and gene expression were found for 115 genes in the time interval 2-4 minutes and for 94 genes in the time interval 4-6 minutes, for which 56 genes were common. This resulted in 153 unique genes for GO and hallmark enrichment analyses (Supplementary Table 3). Two transport-related GO terms were enriched in the list of correlated genes; i.e. intracellular transport and cellular macromolecular localization (**Figure 6**), consistent with a role of transporters in the FACBC

Table 2. Correlation between FACBC uptake (SUVmax) and gene expression level of *ASCT2* and *SNAT2*

Gene symbol	SUVmax 2-4 min		SUVmax 4-6 min	
	rho	*P*	rho	*P*
ASCT2 (SLC1A5)	0.16	0.55	0.21	0.44
SNAT2 (SLC38A2)	0.15	0.57	0.19	0.48
Transporter gene score*	-0.39	0.14	-0.37	0.16

Spearman rank correlation coefficient (rho) and *P*-value are listed. Official gene symbols according to HUGO Gene Nomenclature Committee are shown in parentheses. LAT1 was not assessed because of expression level similar to background noise level. *, Calculated based on the expression of 40 amino acid transporters (**Figure 3**).

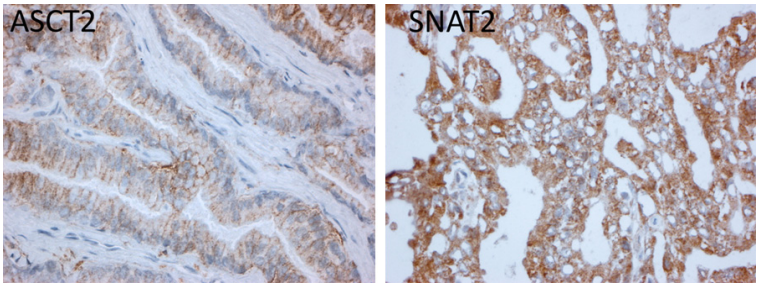

Figure 5. Immunohistochemistry with 40 × enlargement. ASCT2 show mainly membrane staining, with low percentage of the cells in the middle and high percentage in the upper corners. SNAT2 show substantial cytoplasmatic and membrane staining.

uptake. Moreover, we found five hallmarks that were correlated to SUVmax: MYC targets v1, glycolysis, adipogenesis, mTORC1 signalling, and UV response up.

Discussion

In this study, we compared clinical PET imaging with molecular analyses of matched punch biopsies to investigate FACBC uptake mechanisms in prostate cancer patients. While the only previous study performed on patient material focused on the two anticipated essential amino acid transporters ASCT2 and LAT1 [10], we included gene expression data of a comprehensive set of 40 amino acid transporters and protein expression of selected candidates. We further performed whole genome analyses to reveal the biology behind tumors with high FACBC uptake.

LAT1 and ASCT2 are in the FDA-approval document stated as the two main transporters of FACBC into prostate cancer cells. In our study, the gene expression of *LAT1* was barely above background noise level and the protein expression was weak. In a study of 24 patients Saarinen *et al.* found a moderate positive correlation between FACBC uptake *in vivo* and LAT1 [10]. However, this was seen only for higher grade tumors. They further reported that no patients had strong staining intensity and the staining was mainly within the cytoplasm, in accordance with our observations. It is well known that gene expression not always reflects protein expression [5, 15, 16]. This was demonstrated for SNAT2 in our study and was probably a consequence of strong expression in the cytoplasm in addition to the membrane. However, immunohistochemistry of LAT1 did not show staining of the membrane either, only weak staining of the nucleus. The heavy subunit of LAT1, 4F2HC, is essential for a functional LAT1 transporter [17]. Hence, our finding of a strong negative correlation between SUVmax and the gene expression of *4F2HC* further questions LAT1 mediated transport as one of the main uptake mechanisms *in vivo*.

Contrary to LAT1, the gene expression level of *ASCT2* was high and the immunohistochemical staining was strong. However, there was no correlation between FACBC uptake and ASCT2 expression, regardless of whether gene- or protein expression was considered. Similar results were reported by Saarinen *et al*. in their study of 24 patients [10]. However, the lack of correlation does not exclude ASCT2 as a transporter that contributes to FACBC uptake, it rather questions whether ASCT2 is the dominating one. In addition to ASCT2, we found *SNAT1*, *SNAT2*, *PAT1, CAT1, CAT2*, and *LAT2* to be highly expressed. Although none of these showed any relationship to FACBC uptake when analyzed alone, one could speculate if the uptake is mediated by several of the transporters combined. This hypothesis is in line with our global gene analyses, showing association between transport-related GO terms and FACBC uptake. Assessing differences in gene expression

Table 3. Immunoscore for ASCT2 and SNAT2

Patient	ASCT2[a]			SNAT2[b]		
	Staining percentage	Staining intensity	Immuno-score	Staining percentage	Staining intensity	Immuno- score
1	>75	Strong	3 × 3 = 9	<50	Moderate	1 × 2 = 2
2	>75	Strong	3 × 3 = 9	>75	Strong	3 × 3 = 9
3	50-75	Moderate	2 × 2 = 4	>75	Moderate	3 × 2 = 6
4	>75	Strong	3 × 3 = 9	>75	Strong	3 × 3 = 9
5	50-75	Moderate	2 × 2 = 4	50-75	Moderate	2 × 2 = 4
6	>75	Strong	3 × 3 = 9	>75	Strong	3 × 3 = 9
7	>75	Strong	3 × 3 = 9	>75	Strong	3 × 3 = 9
8	<50	Strong	1 × 3 = 3	>75	Strong	3 × 3 = 9
9	>75	Strong	3 × 3 = 9	>75	Strong	3 × 3 = 9
10	>75	Strong	3 × 3 = 9	50-75	Strong	2 × 3 = 6
11	>75	Strong	3 × 3 = 9	>75	Moderate	3 × 2 = 6
12	50-75	Strong	2 × 3 = 6	<50	Moderate	1 × 2 = 2
13	>75	Strong	3 × 3 = 9	>75	Moderate	3 × 2 = 6
14	>75	Strong	3 × 3 = 9	>75	Strong	3 × 3 = 9
15	50-75	Moderate	2 × 3 = 6	<50	Low	1 × 1 = 1
16	>75	Strong	3 × 3 = 9	>75	Strong	3 × 3 = 9

a, Official symbol is *SLC1A5*. b, Official symbol is *SLC38A2*.

Table 4. Correlation between immunoscores, FACBC uptake at PET (SUVmax) and gene expression of ASCT2 and SNAT2

	SUVmax 2-4 min		SUVmax 4-6 min		Gene expression	
	Rho	*P*	Rho	*P*	Rho	*P*
ASCT2 immunoscore	0.31	0.24	0.34	0.20	0.59	0.02
SNAT2 immunoscore	0.13	0.64	0.17	0.54	-0.36	0.17

Spearman rank correlation coefficient (rho) and *P*-value are listed.

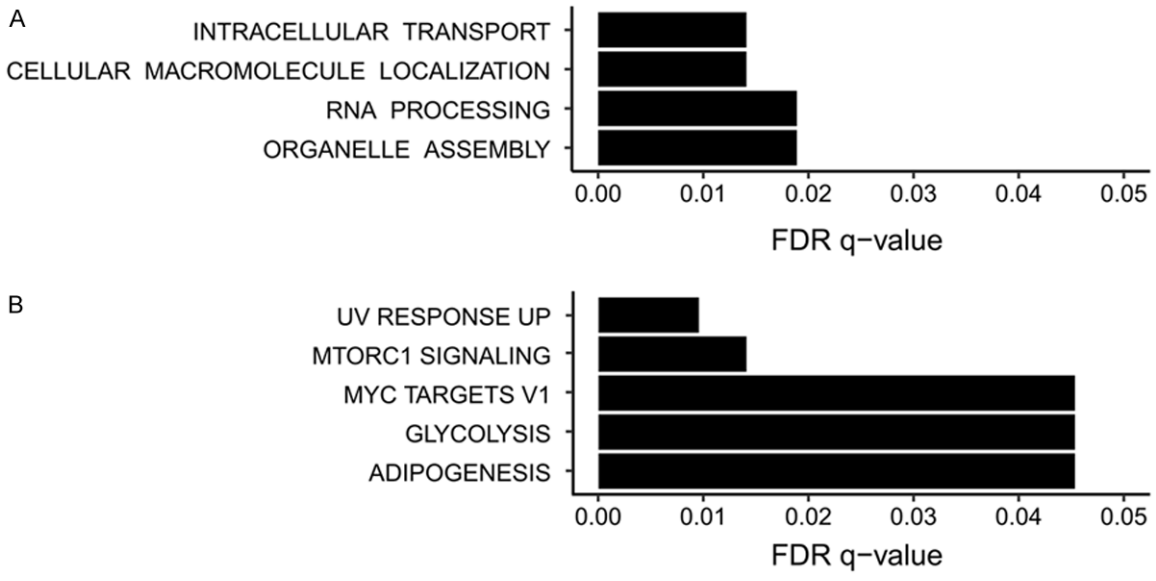

Figure 6. Gene ontology (A) and hallmark (B) enrichment analysis of 153 genes correlated to FACBC uptake (SUVmax) at either 2-4 minutes or 4-6 minutes post injection of FACBC.

between benign and malignant tissues can provide insight into the uptake mechanism of FACBC. We analyzed a publicly available dataset with gene expression data from prostate cancer and normal prostate tissue acquired using the same Illumina-platform (GSE32571). In this dataset the differences in gene expression level of the amino acid transporters between benign and malignant tissues were generally small, mostly non-significant, and sometimes higher in benign tissue and sometimes higher in malignant tissue (Supplementary Table 4). This indicates that FACBC uptake is not mediated by a single amino acid transporter. It further suggests that high FACBC uptake is probably not explained by upregulated gene expression but reflects high metabolic activity in malignant tissue. This is supported by our finding of a relationship between FACBC uptake and hallmarks like glycolysis, MYC targets and mTORC1 signaling, suggesting high metabolic activity and thus, amino acid turnover, in tumors with a high uptake. To further investigate the uptake mechanism, studies using proteomics from prostate tissue with high and low FACBC uptake may improve our understanding.

Our study has some limitations. The patient cohort was small, especially taken into consideration the heterogeneity in tumor aggressiveness, SUVmax and gene expression levels. This might explain why no dominating amino acid transporter appeared to be associated with FACBC uptake in our analyses. Limited spatial resolution of the PET images might have led to suboptimal co-registration between imaging and biopsy location. Furthermore, using clinical PET in which the tumor is reflected by a limited number of voxels, associations found in *in vitro* studies may be undiscovered. Major strengths of the study are the use of clinical material, short time between imaging and surgery, meticulous matching between imaging and histopathology, and a wide range of molecular analyses.

Conclusion

No significant correlations were found between FACBC uptake in primary prostate cancer and the gene expression levels of 40 different amino acid transporters. Global gene expression analyses showed that high FACBC uptake was associated with intracellular transport and high metabolic activity. Our findings indicate that the uptake mechanism of FACBC is more complex than mediated by a few amino acid transporters identified in cell lines studies.

Acknowledgements

Funding was received from the South-Eastern Norway Regional Health Authority (grant number 2016048). The Regional Committee for Medical and Health Research Ethics approved the study and written informed consent was obtained from all patients.

Disclosure of conflict of interest

None.

Address correspondence to: Therese Seierstad, Department of Research and Development, Division of Radiology and Nuclear Medicine, Oslo University Hospital, P. O. Box 4950, Nydalen, Oslo, Norway. Tel: +47 22934000; E-mail: therese@radium.uio.no

References

[1] Shoup TM, Olson J, Hoffman JM, Votaw J, Eshima D, Eshima L, Camp VM, Stabin M, Votaw D and Goodman MM. Synthesis and evaluation of [18F]1-amino-3-fluorocyclobutane-1-carboxylic acid to image brain tumors. J Nucl Med 1999; 40: 331-338.

[2] Okudaira H, Shikano N, Nishii R, Miyagi T, Yoshimoto M, Kobayashi M, Ohe K, Nakanishi T, Tamai I, Namiki M and Kawai K. Putative transport mechanism and intracellular fate of trans-1-amino-3-18F-fluorocyclobutanecarboxylic acid in human prostate cancer. J Nucl Med 2011; 52: 822-829.

[3] Sorensen J, Owenius R, Lax M and Johansson S. Regional distribution and kinetics of [18F] fluciclovine (anti-[18F]FACBC), a tracer of amino acid transport, in subjects with primary prostate cancer. Eur J Nucl Med Mol Imaging 2013; 40: 394-402.

[4] Oka S, Okudaira H, Yoshida Y, Schuster DM, Goodman MM and Shirakami Y. Transport mechanisms of trans-1-amino-3-fluoro[1-(14) C]cyclobutanecarboxylic acid in prostate cancer cells. Nucl Med Biol 2012; 39: 109-119.

[5] Vogel C and Marcotte EM. Insights into the regulation of protein abundance from proteomic and transcriptomic analyses. Nat Rev Genet 2012; 13: 227-232.

[6] Yanagida O, Kanai Y, Chairoungdua A, Kim DK, Segawa H, Nii T, Cha SH, Matsuo H, Fukushima J, Fukasawa Y, Tani Y, Taketani Y, Uchino H, Kim JY, Inatomi J, Okayasu I, Miyamoto K, Takeda E,

Goya T and Endou H. Human L-type amino acid transporter 1 (LAT1): characterization of function and expression in tumor cell lines. Biochim Biophys Acta 2001; 1514: 291-302.
[7] Okudaira H, Nakanishi T, Oka S, Kobayashi M, Tamagami H, Schuster DM, Goodman MM, Shirakami Y, Tamai I and Kawai K. Kinetic analyses of trans-1-amino-3-[18F]fluorocyclobutanecarboxylic acid transport in Xenopus laevis oocytes expressing human ASCT2 and SNAT2. Nucl Med Biol 2013; 40: 670-675.
[8] Sakata T, Ferdous G, Tsuruta T, Satoh T, Baba S, Muto T, Ueno A, Kanai Y, Endou H and Okayasu I. L-type amino-acid transporter 1 as a novel biomarker for high-grade malignancy in prostate cancer. Pathol Int 2009; 59: 7-18.
[9] Fuchs BC and Bode BP. Amino acid transporters ASCT2 and LAT1 in cancer: partners in crime? Semin Cancer Biol 2005; 15: 254-266.
[10] Saarinen I, Jambor I, Kim M, Kuisma A, Kemppainen J, Merisaari H, Eskola O, Koskenniemi AR, Perez IM, Bostrom P, Taimen P and Minn H. Correlation between (18)F-1-amino-3-fluorocyclobutane-1-carboxylic acid ((18)F-fluciclovine) uptake and expression of alanine-serine-cysteine-transporter 2 (ASCT2) and L-type amino acid transporter 1 (LAT1) in primary prostate cancer. EJNMMI Res 2019; 9: 50.
[11] Srigley JR. Key issues in handling and reporting radical prostatectomy specimens. Arch Pathol Lab Med 2006; 130: 303-317.
[12] Sobin LH, Gospodarowicz MK and Wittekind C. TNM classification of malignant tumours. Chichester: Wiley-Blackwell; 2009.
[13] Epstein JI. An update of the Gleason grading system. J Urol 2010; 183: 433-440.
[14] Ragnum HB, Vlatkovic L, Lie AK, Axcrona K, Julin CH, Frikstad KM, Hole KH, Seierstad T and Lyng H. The tumour hypoxia marker pimonidazole reflects a transcriptional programme associated with aggressive prostate cancer. Br J Cancer 2015; 112: 382-390.
[15] Edfors F, Danielsson F, Hallstrom BM, Kall L, Lundberg E, Ponten F, Forsstrom B and Uhlen M. Gene-specific correlation of RNA and protein levels in human cells and tissues. Mol Syst Biol 2016; 12: 883.
[16] Gry M, Rimini R, Strömberg S, Asplund A, Pontén F, Uhlén M and Nilsson P. Correlations between RNA and protein expression profiles in 23 human cell lines. BMC Genomics 2009; 10: 365.
[17] Napolitano L, Scalise M, Galluccio M, Pochini L, Albanese LM and Indiveri C. LAT1 is the transport competent unit of the LAT1/CD98 heterodimeric amino acid transporter. Int J Biochem Cell Biol 2015; 67: 25-33.

Supplementary Table 1. Gene expression levels of amino acid transporters in prostate biopsy specimens from 16 patients

Amino acid transporter	Official gene symbol*	Patient															
		1	2	3	4	5	6	7	8	9	10	11	12	13	14	15	16
TAT1	*SLC16A10*	6.563	6.480	6.954	6.958	6.699	6.939	7.194	6.995	7.130	7.004	6.692	6.967	6.632	6.839	7.419	7.356
EAAT3	*SLC1A1*	7.230	6.487	6.731	6.739	6.911	6.806	8.235	6.670	6.726	6.922	7.121	6.903	7.346	7.038	7.064	6.687
EAAT2	*SLC1A2*	6.807	6.708	6.550	6.663	6.474	6.615	6.715	6.641	6.707	6.548	6.663	6.546	6.811	6.607	6.640	6.641
EAAT1	*SLC1A3*	8.417	6.675	6.975	8.028	7.964	7.260	7.443	7.430	7.408	7.782	7.611	7.946	7.100	7.728	7.920	7.317
ASCT1	*SLC1A4*	7.892	8.330	7.271	7.118	7.025	7.563	8.211	7.609	7.727	7.223	8.497	8.132	7.634	7.486	6.949	7.878
ASCT2	*SLC1A5*	8.294	8.623	8.243	8.423	7.515	8.564	9.538	8.223	8.469	8.630	9.166	9.398	8.746	8.425	8.362	9.186
EAAT4	*SLC1A6*	6.604	6.377	6.599	6.518	6.530	6.556	6.457	6.557	6.505	6.576	6.504	6.540	6.583	6.550	6.654	6.557
EAAT5	*SLC1A7*	6.533	6.917	6.743	6.652	6.789	6.680	6.610	6.688	6.736	6.583	6.778	6.803	6.731	6.635	6.729	6.633
PAT1	*SLC36A1*	8.075	8.110	7.154	7.096	7.215	7.326	7.452	7.122	7.537	7.280	7.319	8.192	8.350	9.052	7.023	8.970
PAT2	*SLC36A2*	6.422	6.579	6.367	6.444	6.444	6.511	6.527	6.401	6.471	6.427	6.502	6.449	6.507	6.524	6.440	6.405
PAT3	*SLC36A3*	6.502	6.477	6.586	6.529	6.414	6.403	6.508	6.502	6.425	6.534	6.479	6.511	6.461	6.450	6.523	6.348
PAT4	*SLC36A4*	6.719	7.193	6.876	6.717	6.650	6.579	6.443	6.641	6.676	6.832	7.154	6.902	6.841	6.942	7.124	6.980
SNAT1	*SLC38A1*	8.620	8.376	9.152	9.082	9.016	8.880	7.498	8.858	8.909	8.982	8.552	9.350	9.117	8.740	8.759	9.431
SNAT2	*SLC38A2*	9.451	8.647	8.694	9.109	7.836	7.993	7.624	7.611	7.720	8.845	8.770	9.237	9.354	8.942	9.513	9.998
SNAT3	*SLC38A3*	6.489	6.589	6.462	6.526	6.530	6.558	6.636	6.602	6.464	6.511	6.567	6.588	6.494	6.534	6.512	6.455
SNAT4	*SLC38A4*	6.574	6.781	6.543	6.566	6.629	6.576	6.499	6.500	6.514	6.522	6.835	6.565	6.787	6.540	6.615	6.551
SNAT5	*SLC38A5*	6.742	6.728	6.658	6.765	6.695	6.773	6.568	6.777	6.828	6.861	6.771	6.743	6.786	6.694	6.826	6.831
SNAT6	*SLC38A6*	7.338	6.789	7.242	7.280	6.730	6.877	6.955	6.711	6.652	6.951	6.976	7.061	7.142	7.125	7.082	7.458
RBAT	*SLC3A1*	6.510	6.446	8.284	6.483	6.721	7.329	6.578	8.512	7.123	7.461	6.625	6.424	6.446	6.687	6.564	6.561
4F2HC	*SLC3A2*	9.332	7.408	8.268	8.239	8.766	8.639	9.842	8.706	8.691	8.601	9.196	9.397	8.895	8.520	8.423	8.560
LAT3	*SLC43A1*	7.638	9.028	7.165	7.098	7.069	7.605	7.982	7.141	7.323	7.501	7.785	7.366	7.173	7.301	7.130	7.124
LAT4	*SLC43A2*	7.107	6.517	6.803	6.881	7.019	6.854	7.286	7.168	7.174	6.912	6.780	7.109	7.195	7.108	7.282	7.104
ATB0+	*SLC6A14*	6.526	6.457	6.528	6.523	6.555	6.510	6.474	6.504	6.480	6.487	6.457	6.494	6.518	6.474	6.429	6.655
B(0)AT2	*SLC6A15*	6.512	6.449	6.389	6.442	6.423	6.456	6.710	6.574	6.432	6.464	6.319	6.500	6.494	6.560	6.500	6.460
B(0)AT1	*SLC6A19*	6.537	6.497	6.535	6.585	6.634	6.597	6.567	6.628	6.677	6.529	6.485	6.592	6.505	6.629	6.527	6.578
SIT1	*SLC6A20*	6.778	8.139	6.661	6.764	6.677	6.752	6.725	6.722	6.799	6.673	6.639	6.754	6.637	6.608	6.652	6.740
GLYT2	*SLC6A5*	6.567	6.510	6.615	6.515	6.562	6.533	6.500	6.603	6.592	6.585	6.594	6.634	6.579	6.642	6.583	6.574
TAUT	*SLC6A6*	6.685	6.553	6.578	6.629	6.691	6.671	6.703	6.601	6.564	6.605	6.641	6.495	6.624	6.577	6.653	6.371
PROT	*SLC6A7*	6.721	7.195	6.645	6.622	6.719	6.667	6.762	6.671	6.667	6.716	6.689	6.651	6.695	6.698	6.768	6.706
GLYT1	*SLC6A9*	6.744	6.886	6.666	6.752	6.673	6.968	6.514	6.771	6.682	6.670	6.886	6.842	6.746	6.761	6.576	6.675
CAT1	*SLC7A1*	9.243	8.586	9.457	9.452	9.426	10.056	10.492	9.455	9.752	10.163	10.188	10.258	9.997	9.566	10.021	9.353
ASC1	*SLC7A10*	6.621	6.381	6.533	6.549	6.540	6.530	6.435	6.570	6.464	6.596	6.447	6.437	6.427	6.542	6.585	6.255
XCT	*SLC7A11*	6.837	6.515	6.455	6.528	6.368	6.485	6.569	6.612	6.396	6.470	6.452	6.468	6.396	6.454	6.446	6.486
CAT2	*SLC7A2*	9.071	6.670	8.293	7.625	8.636	9.018	9.686	8.516	9.347	8.406	8.897	8.563	9.480	8.480	9.093	8.953
CAT3	*SLC7A3*	7.743	6.539	6.863	7.381	7.306	6.890	7.124	6.779	6.681	7.168	6.983	6.788	7.151	6.973	7.243	6.792
LAT1	*SLC7A5*	7.598	6.564	6.868	7.048	7.903	7.009	6.625	6.792	7.124	7.395	6.625	7.446	6.765	6.893	7.059	6.597
Y+LAT2	*SLC7A6*	7.110	6.520	7.037	7.037	7.620	7.296	7.355	7.268	7.276	7.238	6.798	6.921	6.749	7.026	6.973	6.864
Y+LAT1	*SLC7A7*	7.852	6.566	7.134	7.563	7.272	7.164	7.090	7.102	6.948	7.113	7.090	7.368	6.994	7.162	7.257	6.923
LAT2	*SLC7A8*	8.511	8.870	8.490	8.027	8.616	7.981	9.835	8.424	8.065	8.058	9.213	8.660	9.590	7.475	7.824	8.782
BAT1	*SLC7A9*	6.966	7.142	6.631	6.724	6.682	6.618	6.660	6.695	6.922	6.756	7.120	6.667	6.610	6.674	6.755	6.693

Log2-transformed data are listed. *, Official gene symbol according to HUGO Gene Nomenclature Committee.

Supplementary Table 2. Correlation between FACBC uptake at PET (SUVmax) and gene expression level of 40 amino acids

Amino acid transporter	Official gene symbol*	SUVmax 2-4 minutes		SUVmax 4-6 minutes	
		Rho	*P*	Rho	*P*
TAT1	*SLC16A10*	-0.218	0.417	0.347	0.188
EAAT3	*SLC1A1*	0.029	0.917	-0.076	0.780
EAAT2	*SLC1A2*	0.168	0.534	0.029	0.917
EAAT1	*SLC1A3*	-0.412	0.114	-0.421	0.106
ASCT1	*SLC1A4*	-0.129	0.633	-0.018	0.952
ASCT2	*SLC1A5*	0.218	0.417	0.279	0.294
EAAT4	*SLC1A6*	-0.085	0.755	0.141	0.602
EAAT5	*SLC1A7*	0.124	0.648	0.182	0.498
PAT1	*SLC36A1*	-0.068	0.805	0.056	0.839
PAT2	*SLC36A2*	0.479	0.062	0.418	0.109
PAT3	*SLC36A3*	0.050	0.856	0.003	0.996
PAT4	*SLC36A4*	0.300	0.258	0.341	0.196
SNAT1	*SLC38A1*	-0.106	0.697	0.074	0.788
SNAT2	*SLC38A2*	0.141	0.602	0.174	0.519
SNAT3	*SLC38A3*	0.018	0.952	0.018	0.952
SNAT4	*SLC38A4*	0.482	0.061	0.500	0.051
SNAT5	*SLC38A5*	0.109	0.689	0.009	0.978
SNAT6	*SLC38A6*	0.074	0.788	0.200	0.456
RBAT	*SLC3A1*	-0.197	0.463	-0.209	0.436
4F2HC	*SLC3A2*	-0.541	0.033	-0.500	0.051
LAT3	*SLC43A1*	0.188	0.484	0.176	0.512
LAT4	*SLC43A2*	-0.382	0.145	-0.606	0.015
ATB0+	*SLC6A14*	-0.312	0.239	-0.100	0.713
B(0)AT2	*SLC6A15*	-0.324	0.221	-0.429	0.099
B(0)AT1	*SLC6A19*	-0.538	0.034	-0.471	0.068
SIT1	*SLC6A20*	-0.126	0.641	-0.112	0.681
GLYT2	*SLC6A5*	-0.374	0.155	-0.241	0.367
TAUT	*SLC6A6*	0.053	0.848	-0.094	0.730
PROT	*SLC6A7*	0.053	0.848	-0.203	0.450
GLYT1	*SLC6A9*	0.182	0.498	0.391	0.135
CAT1	*SLC7A1*	0.097	0.721	0.065	0.814
ASC1	*SLC7A10*	-0.221	0.410	-0.321	0.226
XCT	*SLC7A11*	-0.162	0.549	-0.097	0.721
CAT2	*SLC7A2*	-0.168	0.534	-0.350	0.184
CAT3	*SLC7A3*	0.068	0.805	-0.024	0.935
LAT1	*SLC7A5*	-0.381	0.145	-0.414	0.111
Y+LAT2	*SLC7A6*	-0.391	0.135	-0.462	0.074
Y+LAT1	*SLC7A7*	-0.232	0.385	0.176	0.512
LAT2	*SLC7A8*	-0.088	0.746	-0.024	0.935
BAT1	*SLC7A9*	-0.047	0.865	-0.144	0.594

Spearman rank correlation coefficient (rho) and *P*-value are listed. *, Official gene symbol according to HUGO Gene Nomenclature Committee.

Supplementary Table 3. Gene Ontology (A) and hallmark (B) enrichment analysis of 153 genes correlated to FACBC uptake (SUVmax) at either 2-4 minutes or 4-6 minutes post injection of FACBC

A

Gene ontology (GO) biological process	Genes	Description	Genes in overlap
Intracellular transport	1758	The directed movement of substances within a cell.	20
Cellular macromolecule localization	1989	Any process in which a macromolecule is transported to. and/or maintained in a specific location at the level of a cell. Localization at the cellular level encompasses movement within the cell, from within the cell to the cell surface, or from one location to another at the surface of a cell.	21
RNA processing	1442	Any process involved in the conversion of one or more primary RNA transcripts into one or more mature RNA molecules.	17
Organelle assembly	878	The aggregation, arrangement and bonding together of a set of components to form an organelle. An organelle is an organized structure of distinctive morphology and function. Includes the nucleus, mitochondria, plastids, vacuoles, vesicles, ribosomes and the cytoskeleton. Excludes the plasma membrane.	13

B

HALLMARK	Genes	Description	Genes in overlap
UV 1 response	158	Genes upregulated in response to ultraviolet radiation	5
mTORC1 signaling	200	Genes upregulated through activation of the mTORC1 complex	5
Adiopogenesis	200	Genes upregulated during adiopocyte differentiation	4
Glycolysis	200	Genes encoding proteins involved in glycolysis and gluconeogenesis	4
MYC targets v1	200	A subgroup of genes regulated by MYC-version 1	4

Supplementary Table 4. Median values of log2-gene expression of amino acid transporters in benign and malignant prostate tissue from the GEO-dataset GSE32571

Amino acid transporter	Benign tissue	Malignant tissue	*P*-value
BAT1 (SLC7A9)	6.75	6.79	0.91
LAT2 (SLC7A8)	8.96	8.86	0.72
Y+LAT1 (SLC7A7)	7.40	7.28	0.18
Y+LAT2 (SLC7A6)	7.07	6.96	0.19
LAT1 (SLC7A5)	7.86	7.48	>0.01
CAT3 (SLC7A3)	6.87	7.04	0.14
CAT2 (SLC7A2)	8.96	8.94	0.64
XCT (SLC7A11)	6.02	6.08	>0.01
ASC1 (SLC7A10)	6.10	6.10	0.86
CAT1 (SLC7A1)	8.86	9.46	>0.01
GLYT1 (SLC6A9)	6.57	6.41	>0.01
TAUT (SLC6A6)	6.03	6.01	0.62
GLYT2 (SLC6A5)	5.85	5.86	0.38
SIT1 (SLC6A20)	6.13	6.16	0.13
B(0)AT1 (SLC6A19)	5.84	5.85	0.95
B(0)AT2 (SLC6A15)	6.15	6.14	0.12
ATB0+ (SLC6A14)	5.96	5.96	0.98
LAT4 (SLC43A2)	6.93	6.78	>0.01
LAT3 (SLC43A1)	6.23	6.59	>0.01
4F2HC (SLC3A2)	6.17	6.44	0.01
RBAT (SLC3A1)	6.03	6.07	0.09
SNAT6 (SLC38A6)	6.21	6.20	0.72
SNAT5 (SLC38A5)	6.34	6.23	0.02
SNAT4 (SLC38A4)	6.06	6.04	0.46
SNAT3 (SLC38A3)	6.08	6.03	0.12
SNAT2 (SLC38A2)	7.76	7.63	0.02
SNAT1 (SLC38A1)	8.50	8.28	>0.01
PAT4 (SLC36A4)	6.76	6.55	>0.01
PAT3 (SLC36A3)	5.88	5.89	0.38
PAT2 (SLC36A2)	5.91	5.91	0.43
PAT1 (SLC36A1)	6.49	6.71	>0.01
EAAT5 (SLC1A7)	6.01	6.05	0.32
EAAT4 (SLC1A6)	*5.85*	*5.84*	*0.14*
ASCT2 (SLC1A5)	*8.84*	*8.71*	*0.64*
ASCT1 (SLC1A4)	*7.56*	*7.62*	*0.10*
EAAT3 (SLCA3)	*7.10*	*6.85*	*>0.01*
EAAT2 (SLC1A2)	*6.01*	*6.03*	*0.40*
EAAT3 (SLC1A1)	*6.63*	*6.65*	*0.58*
TAT1 (SLC16A10)	*6.96*	*7.04*	*0.24*

P-value from Wilcoxon signed-rank test.